Thermodynamic collapse in a lattice-gas model for a two-component system of penetrable particles

Derek Frydel ●

Department of Chemistry, Federico Santa Maria Technical University, Campus San Joaquin, 7820275 Santiago, Chile

Yan Levin

Institute of Physics, The Federal University of Rio Grande do Sul, Porto Alegre 91501-970, Brazil

We study a lattice-gas model of penetrable particles on a square-lattice substrate with same-site and nearest-neighbor interactions. Penetrability implies that the number of particles occupying a single lattice site is unlimited and the model itself is intended as a simple representation of penetrable particles encountered in realistic soft-matter systems. Our specific focus is on a binary mixture, where particles of the same species repel and those of the opposite species attract each other. As a consequence of penetrability and the unlimited occupation of each site, the system exhibits thermodynamic collapse, which in simulations is manifested by an emergence of extremely dense clusters scattered throughout the system with energy of a cluster $E \propto -n^2$, where n is the number of particles in a cluster. After transforming a particle system into a spin system, in the large density limit the Hamiltonian recovers a simple harmonic form, resulting in the discrete Gaussian model used in the past to model the roughening transition of interfaces. For finite densities, due to the presence of a nonharmonic term, the system is approximated using a variational Gaussian model.

I. INTRODUCTION

In a recent article [1] we studied a one-dimensional lattice-gas model of penetrable particles and demonstrated that a two-component system (where particles of the same species repel and those of opposite species attract each other) becomes thermodynamically unstable, where the collapsed state is manifested by the presence of scattered and extremely dense clusters, in which the occupation number of a site that is part of the cluster is $n \gg 1$. This behavior is not unique to lattice models and has been previously observed in more realistic systems of penetrable particles such as a penetrable sphere model [2–4]. Prior to these examples, the possibility of thermodynamic collapse in a multicomponent system of soft particles has been considered as early as 1966 by Ruelle and Fisher [5–7], who also explored mathematical criteria for the conditions in which such a collapse becomes plausible.

The renewed interest in penetrable particles has been triggered by a growing number of synthesized and naturally occurring nanoparticle whose pair interactions lack the usual hard-core repulsion, resulting in ultrasoft particles that interpenetrate and, in principle, can occupy the same space [8]. Penetrability gives rise to different behaviors than those encountered in systems with hard-core repulsion. The type of soft interactions, furthermore, plays a decisive role in determining a particular behavior of the system [9].

In a one-component system, thermodynamic collapse becomes possible for systems with pair interactions composed of a short-range attractive tail and a repulsive soft-core. More recent examples where such systems are studies in connection to thermodynamic collapse include Refs. [10–12], among others. The most famous example of thermodynamic collapse, however, is that in gravitational system [13], whose pair interaction consists of only attractive long-range part. When it comes to two-component systems, a considerably less work has been done to understand the mechanism of thermodynamic collapse.

Thermodynamic collapse in a two-component system is not self-evident, since attractive interactions occur between particles of opposite species, and this implies that a collapsed configuration, or a group of configurations, involves a very specific arrangement of particles whose specific structures has been investigated in Ref. [1] for a one-dimensional lattice-gas model.

Because one-dimensional models, as a general rule, preclude the possibility of a phase transition [14] (interestingly enough, this rule does not apply to thermodynamic collapse), the investigation in the Ref. [1] is not entirely satisfactory. In the present article we consider a binary system on a lattice-square substrate with nearest neighbor interactions, as it is the most standard model in two-dimensions. Because the occupation number is unlimited, the system is closely related to the discrete Gaussian model originally designed to capture the structure and behavior of interfaces and the roughening transition [15–17],

Our results are organized as follows. In Sec. II we introduce the model and write down the corresponding grand partition function. In this section we introduce two distinct ways of counting particles, depending on whether particles are considered as distinguishable or indistinguishable. Different ways of counting particles does not arise for a single occupation lattice-gas models and is a consequence of multiple occupation. In Sec. III we transform the original particle system into spin ensemble. In the transformed ensemble spins

can take on any integer value as a consequence of particle penetrability. In Sec. IV we analyze thermodynamic collapse in the infinite density limit. This limit is the consequence of penetrability and implies that the average occupation of a site is $n \to \infty$. In this limit the Hamiltonian reduces to a harmonic function and the corresponding partition function transforms into a discrete Gaussian model (DG). A similar model was used to study roughening transition of interfaces. In Sec. V we analyze the system at finite density. Due to a nonharmonic term, the resulting partition function is no longer Gaussian and we analyze the system using a Gaussian variational method. Both approximate and exact models indicate the presence of a metastable region, so that even though the global minimum corresponds to a collapsed state, the system remains in metastable equilibrium.

II. THE MODEL

The model consists of two types of particles on a two-dimensional square-lattice substrate. As hard-core interactions are not included, there is no restriction on the number of particles that can occupy a single site. If the occupation numbers for a given site are n_i^+ and n_i^-, where the superscripts "+" and "−" designates different species, then the Hamiltonian of the system is

$$H = K \sum \left[\frac{1}{2} n_i^+(n_i^+ - 1) + \frac{1}{2} n_i^-(n_i^- - 1) - n_i^+ n_i^- \right]$$
$$+ \alpha K \sum_{nn} [n_i^+ n_j^+ + n_i^- n_j^- - n_i^+ n_j^- - n_i^- n_j^+], \quad (1)$$

where the first line is for the interaction between particles on the same site, and the second line is for the interaction between particles on neighboring sites (the subscript *nn* indicates the nearest-neighbor interaction). The dimensionless coupling parameter α for interactions between neighbors is positive in our model. This implies that particles of opposite species attract and those of the same species repel each other.

The fact that each lattice site can be occupied by multiple particles at one time results in two types of statistics. If particles are distinguishable as in classical fluids, then the grand canonical partition function is

$$\Xi_a = \sum_{n_1^+=0}^{\infty} \sum_{n_1^-=0}^{\infty} \cdots \sum_{n_N^+=0}^{\infty} \sum_{n_N^-=0}^{\infty} e^{-\beta H_{\text{int}}} \prod_{i=1}^{N} \frac{e^{\beta \mu'(n_i^+ + n_i^-)}}{n_i^+! n_i^-!}, \quad (2)$$

where

$$H_{\text{int}} = \frac{K}{2} \sum (n_i^+ - n_i^-)^2 + \alpha K \sum_{nn} (n_i^+ - n_i^-)(n_j^+ - n_j^-) \quad (3)$$

is the interaction Hamiltonian,

$$\mu' = \mu + \frac{K}{2} \quad (4)$$

is the effective chemical potential, and $N = L^2$ is the number of lattice sites, where L is the size of the system. The factor $1/n_i!$, also referred to as the Gibbs correction, is a feature of distinguishable particles, and indicates that statistics at a single site follows a poisson rather than an exponential distribution. A more detailed analysis of distinguishability versus indistinguishability is provided in Ref. [1].

However, if particles are regarded as indistinguishable, then a situation which in classical systems arises for example in growth models, where particles do not change their location on the lattice substrate but rather are added or removed from it at each Monte Carlo step, in which case the particles of a given site have no labels, then the grand partition function is

$$\Xi_b = \sum_{n_1^+=0}^{\infty} \sum_{n_1^-=0}^{\infty} \cdots \sum_{n_N^+=0}^{\infty} \sum_{n_N^-=0}^{\infty} e^{-\beta H_{\text{int}}} \prod_{i=1}^{N} e^{\beta \mu'(n_i^+ + n_i^-)}. \quad (5)$$

Based on the above discussion, even if the systems obey the same Hamiltonian, they can be subject to different rules of statistical mechanics which, in turn, can lead to different behaviors. This difference can be particularly relevant in characterizing thermodynamic collapse. As this issue does not arise in a standard lattice-gas model with occupations limited to one, it is important to emphasize it as well as consider it in overall analysis.

III. TRANSFORMATION INTO A SPIN-ENSEMBLE

The system described above can be simplified by transforming it into a spin ensemble with spins corresponding to $s_i = n_i^+ - n_i^-$. Because a single configuration in the spin-ensemble corresponds to infinitely many configurations in the particle-ensemble, these degeneracies need to be correctly accounted for. The resulting transformed partition functions are [1]

$$\Xi_a = \sum_{s_1=-\infty}^{\infty} \cdots \sum_{s_N=-\infty}^{\infty} e^{-\beta K \alpha \sum_{nn} s_i s_j} \prod_{i=1}^{N} \left[e^{-\frac{\beta K}{2} s_i^2} I_{s_i}(2e^{\beta \mu'}) \right], \quad (6)$$

and

$$\Xi_b = \sum_{s_1=-\infty}^{\infty} \cdots \sum_{s_N=-\infty}^{\infty} e^{-\beta K \alpha \sum_{nn} s_i s_j} \prod_{i=1}^{N} \left[e^{-\frac{\beta K}{2} s_i^2} \frac{e^{\beta \mu'|s_i|}}{1 - e^{2\beta \mu'}} \right], \quad (7)$$

for distinguishable and indistinguishable particles, respectively. The terms inside square brackets can be regarded as effective external field. Furthermore, as these terms are even function in s_i, the spin symmetry is never broken so that $\langle s_i \rangle = 0$ under all conditions. The function $I_s(x)$ in Eq. (6) is the modified Bessel function of the first kind.

Any quantity defined in the original ensemble can be calculated as another quantity in the spin-ensemble. For example, the average number of particles at a single site i, in the original ensemble defined as

$$\rho_i = \langle n_i^+ \rangle + \langle n_i^- \rangle = \frac{1}{N} \frac{\partial \ln \Xi}{\partial \beta \mu}, \quad (8)$$

in the spin-ensemble becomes

$$\rho_i = e^{\beta \mu'} \left\langle \frac{I_{s_i+1}(2e^{\beta \mu'}) + I_{s_i-1}(2e^{\beta \mu'})}{I_{s_i}(2e^{\beta \mu'})} \right\rangle_s, \quad (9)$$
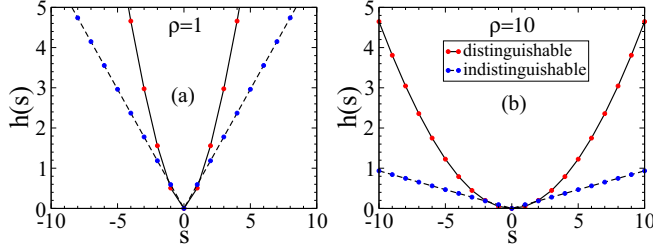
FIG. 1. The functions $h(s)$ for distinguishable and indistinguishable particles for $\beta K = 5$ and $\alpha = 1/4$ and for two different densities, see Eq. (14). For $\rho = 1$ in (a), $\beta\mu' = -0.27$ and $\beta\mu' = -0.57$, and for $\rho = 10$ in (b), $\beta\mu' = 1.66$ and $\beta\mu' = -0.09$ for distinguishable and indistinguishable particles, respectively.

for distinguishable particles, where the subscript s indicates the average calculated in the spin ensemble, and

$$\rho_i = \langle |s_i| \rangle_s + \frac{2e^{2\beta\mu'}}{1 - e^{2\beta\mu'}}, \tag{10}$$

for indistinguishable particles. For distinguishable particles, the limit $\rho_i \to \infty$ is attained if $\mu' \to \infty$, and for indistinguishable particles if $\mu' \to 0^-$. In the rest of the paper, we use $\rho \equiv \rho_i$, to indicate the average number of particles on any lattice site and refer to ρ as density. The limit $\rho \to \infty$ is a consequence of the fact that no limit is placed on the occupation number. This is quite different from the standard lattice-gas model where the maximum density is $\rho = 1$.

The spin-ensembles in Eqs. (6) and (7) more generally can be written as

$$\Xi = B^N \sum_{s_1 = -\infty}^{\infty} \cdots \sum_{s_N = -\infty}^{\infty} e^{-\beta H}, \tag{11}$$

with the prefactors

$$B(\mu') = \begin{cases} I_0(2e^{\beta\mu'}), & \text{distinguishable,} \\ \frac{1}{1 - e^{2\beta\mu'}}, & \text{indistinguishable,} \end{cases} \tag{12}$$

and the Hamiltonian is given by

$$H = \alpha K \sum_{nn} s_i s_j + \frac{K}{2} \sum s_i^2 + \sum h(s_i), \tag{13}$$

where the one-body potentials $h(s_i)$ are

$$\beta h(s_i) = \begin{cases} -\ln\left[\frac{I_{s_i}(2e^{\beta\mu'})}{I_0(2e^{\beta\mu'})}\right], & \text{distinguishable,} \\ -\beta\mu'|s_i|, & \text{indistinguishable.} \end{cases} \tag{14}$$

Note that in the limit $\rho \to \infty$, $h(s_i) \to 0$ and both Hamiltonians become a simple harmonic function. The difference between distinguishable and indistinguishable particles, therefore, becomes relevant at finite densities. For illustration and to see how these differences might be manifested, in Fig. 1 we plot $h(s)$ for distinguishable and indistinguishable particles for the parameters $\beta K = 5$ and $\alpha = 1/4$. Based on the figure, one may expect larger fluctuations for indistinguishable particles due to the shape of the function $h(s_i)$.

A. Connection with other spin models

It might be of interest to place our spin model in the context of other related models. The first difference to be noted is that unlike the standard Ising model, our model permits a spin $s_i = 0$, which can be regarded as an empty site. The class of Ising models that permit empty sites are referred to as site-diluted Ising models with the Hamiltonian $H = -J \sum_{nn} p_i p_j s_i s_j$, where $s_i = \pm 1$ and $p_i = 0, 1$ are random (correlation free) occupation numbers such that $\langle p_i \rangle = \rho$ [18,19]. These models assume the presence of defects in the lattice structure in a magnetic material and represent quenched dilution. Models describing annealed dilution are possible and have been studied in the past [20]. Our model can be regarded as a version of a site-diluted (annealed) model, which would be interesting to study in its own right by limiting spins to $s_i = -1, 0, 1$, where the frequency of empty spins is determined by the function $h(s_i)$.

Our model bears the closest analogy to the discrete Gaussian model (DG) [15,21] dubbed so by Chui and Weeks in 1976. The DG model belongs to a family of random surface models and whose Hamiltonian is given by $H = \frac{1}{2} J \sum_{nn}(s_i - s_j)^2 + 4hJ \sum_n s_i^2$. In the limit $\rho \to \infty$, where $h(s) = 0$, our model corresponds to the DG model. For the parameter $h = 0$, the DG model can be mapped onto a lattice Coulomb system, and like the lattice Coulomb model, it exhibits the Kosterlitz-Thouless transition. This corresponds to our parameter $\alpha = 1/4$. Appendix D shows the equivalence between the Chui-Weeks and the present model.

B. Simulation details

In addition to analytical results, we study the transformed spin ensemble using Monte Carlo simulation. The simulated system consists of spins on a square-lattice substrate. A simulation box itself is a square of size $L = 128$ with periodic boundary conditions. A Monte Carlo move consists of a random selection of a lattice site followed by the trial change of the spin by either 1 or -1 with equal probability. The move is accepted if it lowers the energy, otherwise it is accepted with the probability $e^{-\beta(H_{\text{new}} - H_{\text{old}})}$. Before calculating average quantities, the system is equilibrated for half a million steps. The average quantities are subsequently computed during another 2 million steps.

IV. THE LIMIT $\rho \to \infty$

In the limit $\rho \to \infty$, $h(s_i)$ as defined in Eq. (14) vanishes and the Hamiltonian in Eq. (13) for both distinguishable and indistinguishable particles attains a simple quadratic form

$$H_\infty = \alpha K \sum_{nn} s_i s_j + \frac{K}{2} \sum s_i^2, \tag{15}$$

whose Boltzmann factor is a Gaussian function and, as the spins are restricted to integers, the resulting system is a discrete Gaussian model (DG). In the past, the DG model has been used to model an interface [15–17]. Although the interpretation and the parametrization of that DG model for interfaces is different from ours (in the interface model spins represent height of an interface and, as the heights of neighboring spins tend to be the same, $\alpha < 0$), the same general

analysis applies to both. The analogy between the interface model and the present binary lattice-gas system of penetrable particles is also interesting.

Even though the partition function of the DG model has a Gaussian form, it cannot be solved exactly. However, if we neglect spin discreteness, then it may be possible to approximate the DG model with the continuous Gaussian model (CG) which can be solved exactly [22,23].

A systematic way to carry this out is to write the partition function for the DG model where the partition function of the CG model is a contributing term. Any additional term would then represent contributions due to spin discreteness. To see if this can be done, we first reformulate the Hamiltonian in Eq. (15) using matrix notation,

$$H_\infty = \frac{K}{2} \sum_{i,j} A_{ij} s_i s_j = \frac{K}{2} s^T A s, \qquad (16)$$

where $s = (s_1, \ldots, s_N)$ is the N-dimensional vector, A is a $N \times N$ matrix with elements

$$A_{ij} = \delta_{ij} + \alpha \epsilon_{ij}, \qquad (17)$$

where δ_{ij} is the Kronecker δ function, and $\epsilon_{ij} = 1$ if the two spins are the nearest neighbors and zero otherwise. A for an arbitrary dimension d is given in Appendix B. The corresponding partition function is

$$\Xi_\infty = \sum_{s_1=-\infty}^{\infty} \cdots \sum_{s_N=-\infty}^{\infty} e^{-\frac{\beta K}{2} s^T A s}. \qquad (18)$$

Note that we ignore the pre-factor B defined in Eq. (12) which in the limit $\rho \to \infty$ diverges, however, regardless of its value, it does not affect configurations.

If we rewrite the partition function in Eq. (18) as

$$\Xi_\infty = \prod_{i=1}^{N} \int_{-\infty}^{\infty} ds_i \sum_{n_i=-\infty}^{\infty} \delta(s_i - n_i) \, e^{-\frac{\beta K}{2} s^T A s}, \qquad (19)$$

and express the Dirac comb function as a Fourier series,

$$\sum_{n=-\infty}^{\infty} \delta(s-n) = \sum_{k=-\infty}^{\infty} e^{i2\pi k s}, \qquad (20)$$

then we arrive at

$$\Xi_\infty = \sum_{k_1=-\infty}^{\infty} \cdots \sum_{k_N=-\infty}^{\infty} \\ \times \left[\int_{-\infty}^{\infty} ds_1 \cdots \int_{-\infty}^{\infty} ds_N \, e^{i2\pi \mathbf{k} \cdot \mathbf{s}} e^{-\frac{\beta K}{2} s^T A s} \right], \quad (21)$$

where the integral term in square brackets is a Gaussian integral with a linear term that can be evaluated exactly using the identity

$$\int d\mathbf{x} \, e^{i\mathbf{k}\cdot\mathbf{s}} e^{-\frac{1}{2} s^T A s} = e^{-\frac{1}{2} k^T A^{-1} k} \sqrt{\frac{(2\pi)^N}{\det A}}, \qquad (22)$$

where A^{-1} is the inverse of the matrix A. The resulting partition function is composed of two subsystems,

$$\Xi_\infty = \Xi_G \Xi_L, \qquad (23)$$

where Ξ_G is the partition function of the CG model,

$$\Xi_G = \left(\frac{2\pi}{\beta K} \right)^{N/2} \sqrt{\frac{1}{\det A}}, \qquad (24)$$

and Ξ_L represents all the contributions due to spin discreetness and is given by

$$\Xi_L = \sum_{s_1=-\infty}^{\infty} \cdots \sum_{s_N=-\infty}^{\infty} e^{-\frac{1}{2} \frac{1}{\beta K/(4\pi^2)} s^T A^{-1} s}, \qquad (25)$$

The dimensionless temperature of Ξ_L is $k_B T' = \beta K/(4\pi^2)$.

A. Continuous Gaussian model

From Eq. (23) it is seen that by approximating the DG model as

$$\Xi_\infty \approx \Xi_G,$$

the missing contributions due to the spin discreteness are contained in the term Ξ_L. In this section we verify how accurate this approximation is. To do this, we need to evaluate Ξ_G.

The determinant in Eq. (24) is solved using the identity

$$\det A = \prod_{k=1}^{N} \lambda_k, \qquad (26)$$

where λ_k are the eigenvalues of A. A is a circulant block matrix with circulant blocks [24–26]. The eigenvalues of a circulant matrix are Fourier modes. For a matrix A in $d = 2$ the eigenvalues are

$$\lambda(q_1, q_2) = 1 + 2\alpha \cos q_1 + 2\alpha \cos q_2, \qquad (27)$$

where

$$q_i = \frac{2\pi n_i}{L}, \quad n_i = 0, 1, \ldots, L-1, \qquad (28)$$

so that in total there are $N = L^2$ eigenvalues. The determinant of A now becomes

$$\det A = e^{\sum_{n_1=0}^{L-1} \sum_{n_2=0}^{L-1} \ln[1+2\alpha \cos(\frac{2\pi}{N} n_1)+2\alpha \cos(\frac{2\pi}{N} n_2)]}, \qquad (29)$$

which in the thermodynamic limit $L \to \infty$ becomes

$$\det A = e^{(\frac{L}{2\pi})^2 \int_0^{2\pi} dq_1 \int_0^{2\pi} dq_2 \, \ln[1+2\alpha \cos q_1 + 2\alpha \cos q_2]}. \qquad (30)$$

To complete the expression, it remains to evaluate the integral

$$I = \left(\frac{1}{2\pi} \right)^2 \int_0^{2\pi} dq_1 \int_0^{2\pi} dq_2 \, \ln[1 + 2\alpha \cos q_1 + 2\alpha \cos q_2]. \qquad (31)$$

When evaluated, it corresponds to a hypergeometric function which can also be expressed as a power series in α,

$$I = -\sum_{k=1}^{\infty} \frac{\alpha^{2k}}{2k} \frac{(2k)!^2}{k!^4}. \qquad (32)$$

The interval of convergence of the above series is $|\alpha| \leqslant 1/4$. At $\alpha = 1/4$, I remains finite with a value $I \approx -0.220$. For any value outside the radius of convergence, the series diverges, which in the present model implies thermodynamic instability. We designate this value of α as α_c.
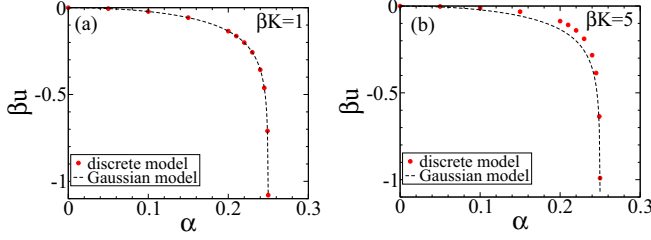
FIG. 2. The internal energy u as a function of α for (a) $\beta K = 1$ and (b) $\beta K = 5$. The data points of a discrete Gaussian model are obtained from Monte Carlo simulation with $L = 128$, and the dashed lines correspond to Eq. (37).
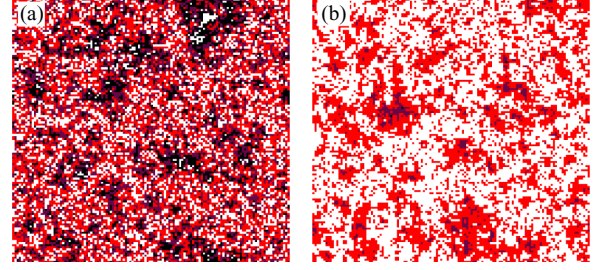

FIG. 3. Configuration snapshot for $\alpha = 0.2499$, for (a) $\beta K = 1$ and (b) $\beta K = 5$. The zero spins are regarded as empty sites and are represented by unfilled squares. Red is for spins $s_i = \pm 1$, purple for $s_i = \pm 2$, and black for $s_i = \pm 3, \pm 4, \dots$.

Given the above results, the partition function in Eq. (24) becomes

$$\Xi_G = \left(\frac{2\pi}{\beta K}\right)^{N/2} \exp\left[\frac{N}{4}\sum_{k=1}^{\infty}\frac{\alpha^{2k}}{k}\frac{(2k)!^2}{k!^4}\right]. \qquad (33)$$

It is interesting to consider at this point the partition function of the Ising model that can be expressed as (see Appendix C)

$$\Xi_{IS} = [2\cosh(2\beta J)]^N \exp\left[-\frac{N}{4}\sum_{k=1}^{\infty}\frac{\alpha^{2k}}{k}\frac{(2k)!^2}{k!^4}\right], \qquad (34)$$

where α is a function of βJ according to

$$\alpha = \frac{1}{2}\frac{\sinh(2\beta J)}{\cosh^2(2\beta J)}, \qquad (35)$$

and J is the interaction strength between nearest neighbor sites. In both the DG and the Ising model the value $\alpha = 1/4$ has physical significance. In the Ising model it indicates a critical point of a continuous phase transition and in the Gaussian model it is the last point before thermodynamic instability. The Ising model, however, is prevented from leaving the convergence region as a result of the parametrization in Eq. (35), and thermodynamic instability never precipitates.

Going back to the partition function Ξ_G, we point out that even if Ξ_G is finite at α_c other quantities may diverge. The internal energy defined as

$$\beta u = -\frac{\alpha}{N}\frac{\partial \log \Xi_G}{\partial \alpha} = 2\alpha K\langle s_i s_j\rangle, \qquad (36)$$

where $\langle s_i s_j\rangle$ are spin correlations between two nearest neighbors, can be calculated exactly using Eq. (33), leading to

$$\beta u(\alpha) = \frac{1}{2} - \frac{1}{\pi}\mathrm{K}(16\alpha^2), \qquad (37)$$

where $\mathrm{K}(x)$ is the complete elliptic integral of the first kind, which contains logarithmic singularity at α_c,

$$\beta u(\alpha) \approx \frac{1}{2} + \frac{1}{2\pi}\ln\left(\frac{1-4|\alpha|}{8}\right). \qquad (38)$$

In Fig. 2 we plot βu. The data points are from the Monte Carlo simulation for the system Ξ_∞ and the dashed line corresponds to the expression in Eq. (37). For $\beta K = 1$, the data points follow closely the continuous Gaussian model. For larger βK, the two results diverge, yet despite this the point of thermodynamic instability is the same for both models.

In Fig. 3 we show configuration snapshots close to thermodynamic collapse (at $\alpha = 0.2499$) for different values of K. The spin $s_i = 0$ is regarded as an empty site, and the colored squares are for $s_i \neq 0$.

The same configurations are shown in Fig. 4 but in a way as to emphasize their antiferromagnetic order. Red squares are for positive and black squares for negative spins. In both cases, configurations appear as islands of antiferromagnetic material immersed in disordered low density phase. For $\beta K = 1$, the islands are much larger and appear interconnected, while for $\beta K = 5$ the islands are separated, reminiscent of the liquid-gas coexistence.

Another revealing quantity is the distribution of spins at a single site $p(s)$. For the continuous Gaussian model such a distribution is expected to be Gaussian (see Appendix B for details),

$$p(s) = \frac{e^{-s^2/2\sigma^2}}{\sqrt{2\pi\sigma^2}}. \qquad (39)$$

The variance can be obtained by knowing that the total energy per particle for a harmonic system is $\beta u_{\text{tot}} = 1/2$. The two contributions to the total energy are $\beta u_{\text{tot}} = \beta u + \beta u_{\text{ext}}$, where $\beta u_{\text{ext}} = \int_{-\infty}^{\infty} ds\, p(s)K s^2/2$ and βu is given in Eq. (37). This leads to the following result:

$$\sigma^2 = \frac{2\mathrm{K}(16\alpha^2)}{\pi\beta K}, \qquad (40)$$
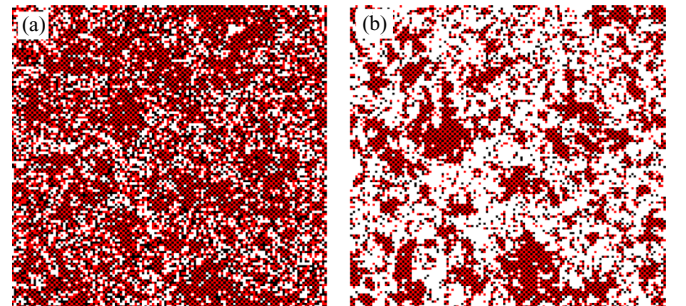

FIG. 4. Configuration snapshot as in Fig. 3 plotted to emphasize "antiferromagnetic" order of the configurations. The empty sites appear as unfilled squares. The remaining spins appear as red squares if $s_i > 0$ and as black squares if $s_i < 0$.
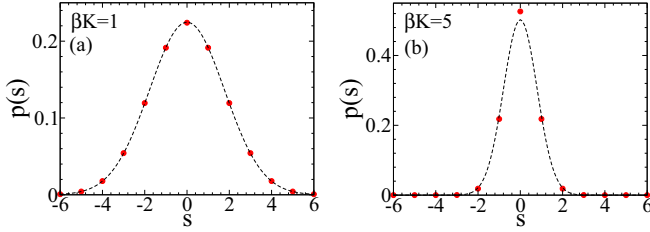
FIG. 5. Distributions $p(s)$ for $\alpha = 0.2499$, and $\beta K = 1$ in (a) and $\beta K = 5$ in (b). The discrete points are from a simulation and the continuous lines correspond to Eq. (39).

and in the limit $\alpha \rightarrow \alpha_c$ we have

$$\sigma^2 = \langle s^2 \rangle \approx -\frac{1}{\pi \beta K} \ln \left(\frac{1 - 4|\alpha|}{8} \right). \quad (41)$$

In Fig. 5 we plot the distributions $p(s)$ for $\alpha = 0.2499$, for different values of βK, and compare the results with the distribution in Eq. (39). For $\beta K = 1$, the discrete data points coincide with the continuous results.

B. Discrete subsystem Ξ_L

In the previous section we approximated the Ξ_∞ system by neglecting its spin discreteness, and the comparison with the simulation showed that such approximation is generally correct for $\beta K < 5$, and even if not correct at every point, the CG model correctly predicts the point of thermodynamic collapse, suggesting that discreteness has no effect on the thermodynamic collapse. The explanation for this is that close to instability the variance of the distribution $p(s)$ diverges, and for large spin variations the spin discreteness becomes irrelevant.

In this section we look more carefully into the neglected contributions of spin discreteness by looking into the behavior of Ξ_L. According to Ref. [15], the DG model at $\alpha = \alpha_c$ is isomorphic with the lattice Coulomb model which exhibits the Kosterlitz-Thouless (KT) transition. This means that at precisely the point where our system is about to collapse, the system also undergoes the KT transition along the parameter βK [27]. This by itself cannot affect the collapse transition; however, it can modify the manner of that collapse.

1. Ξ_L in one dimension

To establish the procedure in a clear manner, we consider first a simpler case of a system in $d = 1$, for which the matrix A is given in Eq. (B1) and the matrix A^{-1} is

$$A_{ij}^{-1} = \frac{1}{L} \sum_{k=0}^{L-1} \frac{\cos[2\pi k(i-j)/L]}{1 + 2\alpha \cos(2\pi k/L)}. \quad (42)$$

Because the value of α_c depends on dimensionality according to $\alpha_c = 1/(2d)$, in $d = 1$ thermodynamic collapse occurs for $\alpha_c = 1/2$.

In the limit $L \rightarrow \infty$ the summation in Eq. (42) becomes an integral,

$$A_{ij}^{-1} = \frac{1}{2\pi} \int_0^{2\pi} dq \frac{\cos[q(i-j)]}{1 + 2\alpha \cos(q)}, \quad (43)$$

which evaluates to

$$A_{ij}^{-1} = \frac{(-1)^{|i-j|}}{\sqrt{1 - 4\alpha^2}} \left(\frac{1 - \sqrt{1 - 4\alpha^2}}{2\alpha} \right)^{|i-j|}. \quad (44)$$

At α_c, A_{ij}^{-1} diverges, but the divergence can be subtracted and the system can be analyzed in terms of nondivergent interactions. To do this, we introduce an alternating sign matrix,

$$C_{ij} = (-1)^{|i-j|}, \quad (45)$$

then subtract from each element A_{ij}^{-1} the divergent term $C_{ij}/\sqrt{1 - 4\alpha^2}$. The remaining elements constitute an interaction matrix $U_{ij} = A_{ij}^{-1} - C_{ij}/\sqrt{1 - 4\alpha^2}$, which at $\alpha = \alpha_c$ reduces to

$$U_{ij} = -(-1)^{|i-j|}|i - j|. \quad (46)$$

The Hamiltonian of the system Ξ_L can now be written as

$$\beta H_L = \frac{2\pi^2}{\beta K} \left[s^T U s + \frac{s^T C s}{\sqrt{1 - 4\alpha^2}} \right]. \quad (47)$$

Clearly, only configurations which suppress the divergence are allowed. Such configurations satisfy $s^T C = 0$, which is the same as

$$\sum_{\text{odd}} s_i = \sum_{\text{even}} s_i, \quad (48)$$

where the subscripts "odd" and "even" refer to odd and even numbered lattice sites. Taking this restriction into account, the Hamiltonian can now be written as

$$\beta H_L' = \frac{2\pi^2}{\beta K} s^T U s, \quad (49)$$

where the prime implies the restriction in Eq. (48).

Although not immediately clear, Ξ_L is an even function of α, and flipping the sign of α does not change the partition function. [The sign change modifies Eq. (44), but as the summations in Ξ_L are over $s_i \in (-\infty, \infty)$, this does not effect the value of Ξ_L]. Calculations then can equally be done for $\alpha = -1/2$. In such a case, the interaction potential becomes

$$U_{ij} = -|i - j|, \quad (50)$$

which is a Coulomb interaction in 1D. There are two differences between the present system and the more usual Coulomb model, however. First, the valance number of particles on a lattice site is unlimited. Second, the periodic boundary conditions involve only particles in the simulation box and do not include contributions due to images outside the original simulation box.

2. Ξ_L in two dimensions

Based on the results of the previous section for $d = 1$, it is guessed that in $d = 2$ the interactions between lattice sites are logarithmic at α_c, since this is the functional form of Coulomb interactions in this dimension. It is more convenient to represent interactions between spins on a square-lattice, not in terms of the matrix A^{-1}, but in terms of a pair potential between sites on the (x, y)-grid, and such a potential would
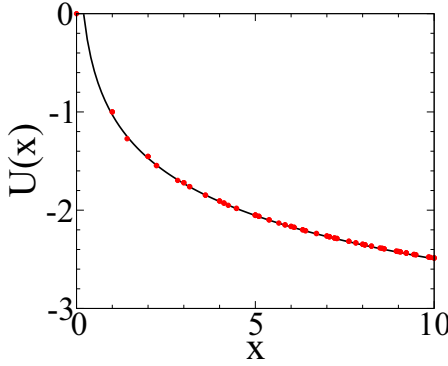
FIG. 6. Approximate pair potential in Eq. (55) compared to the exact results in Eq. (54) at discrete locations on a square-lattice.

have the following form [15]:

$$U_{\text{tot}} = \left(\frac{1}{2\pi}\right)^2 \int_{-\pi}^{\pi} dq_1 \int_{-\pi}^{\pi} dq_2 \frac{\cos(q_1 n + q_2 m)}{1 + 2\alpha\cos(q_1) + 2\alpha\cos(q_2)},$$
(51)

where $n = |x_1 - x_2|$ and $m = |y_1 - y_2|$ indicate a separation between two lattice sites on the discrete Cartesian grid, where $x_i, y_i = 0, 1, \ldots$. The expression is analogous to that in Eq. (43) for $d = 1$ in the limit $L \to \infty$.

If we expand the integrand in powers of α and then evaluate each term, then we find the following series expansion:

$$U_{\text{tot}}(m, n) = \sum_{k=0}^{\infty} \frac{(-1)^{m+n}\alpha^{2k+m+n}(2k+m+n)!^2}{k!(k+m)!(k+n)!(k+m+n)!}, \quad (52)$$

which constitutes a hypergeometric function. $U_{\text{tot}}(m, n)$ diverges at $\alpha_c = 1/4$, and the divergent term is identified as

$$U_{\text{tot}}(0, 0) = \frac{2\text{K}(16\alpha^2)}{\pi}, \quad (53)$$

where K(x) is the complete elliptic integral of the first kind. Subtracting the divergence from U_{tot}, the nondivergent pair potential is

$$U(m, n) = U_{\text{tot}}(m, n) - (-1)^{m+n}\frac{2\text{K}(16\alpha^2)}{\pi}, \quad (54)$$

where an accurate approximation to $U(m, n)$ at α_c is [28]

$$U(m, n) \approx -(-1)^{m+n}\frac{2}{\pi}\left(\ln\sqrt{n^2 + m^2} + \gamma + \frac{1}{2}\ln 8\right), \quad (55)$$

which is valid for $\sqrt{n^2 + m^2} \geqslant 1$. For $n = m = 0$ we use $U = 0$. The approximate functional form in Eq. (55) compared with the exact form in Eq. (54) is shown in Fig. 6.

Because the constant terms in $U(m, n)$, together with the divergent term, are irrelevant, the pair interaction can simply be written as

$$U = -(-1)^{m+n}\frac{2}{\pi}\ln\sqrt{n^2 + m^2}. \quad (56)$$

The spin configurations are subject to the same restriction as that in Eq. (48). In the square-lattice setting, this means that the lattice is decomposed into two interpenetrating sublattices and the restriction amounts to $\sum_{\text{sub}_1} s_i = \sum_{\text{sub}_2} s_i$.
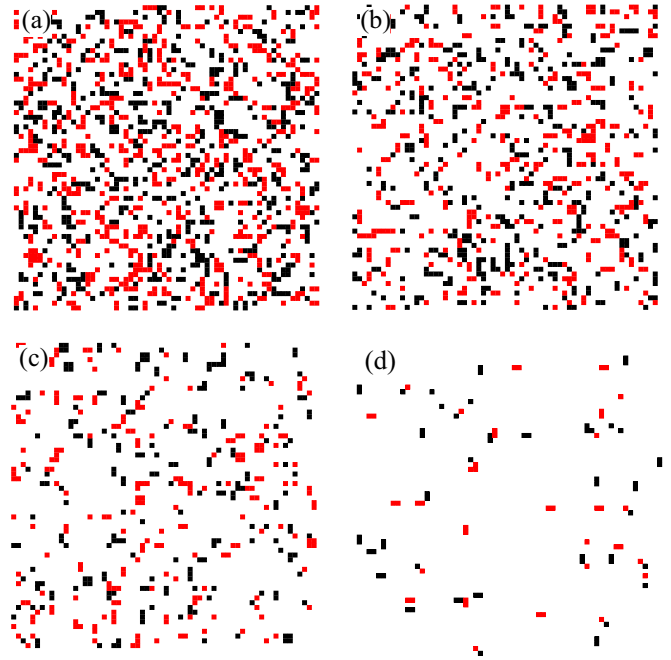

FIG. 7. Configuration snapshots for Ξ_L at α_c for different values of βK, $\beta K = 12, 10, 8, 6$. Red squares are for $s = 1$, black squares for $s = -1$, and the white squares represent empty sites. Spins larger than 1 are negligible for those values of βK that are plotted. The system size is $L = 64$.

The Hamiltonian at α_c can be written as

$$\beta H_L' = -\frac{4\pi}{\beta K}\sum_{x_1, y_1 = 1}^{L}\sum_{x_2, y_2 = 1}^{L}(-1)^{m+n}s_{x_1, y_1}s_{x_2, y_2}\ln\sqrt{n^2 + m^2},$$
(57)

with x_i and y_i indicating discrete locations on a lattice grid.

In Fig. 7 we show several configuration snapshots of Ξ_L for decreasing values of βK. One observes gradual decrease of spin density with decreasing βK, and for $\beta K = 6$ the configuration consists of sparse isolated spins or spin pairs of the same sign. This means that for $\beta K < 6$, $\Xi_L \approx 1$ since most likely value of a spin is $s_i = 0$.

The distribution of spins $p(s)$ is accurately represented using the continuous Gaussian approximation, see Appendix A, given by

$$p(s) = e^{-2\pi^2 s^2/\beta K}\sqrt{\frac{2\pi}{\beta K}}, \quad (58)$$

where the spin variance is given by $\langle s^2 \rangle = \frac{\beta K}{4\pi^2}$. Figure 8 compares the above Gaussian distribution with the discrete distributions obtained from simulation, showing a general good agreement between the two.

The Gaussian distribution in Eq. (58), however, cannot be a reliable approximation of the discrete system if $p(0) > 1$, since this implies that the probability that a spin is zero is greater than one. The Gaussian approximation in Eq. (58), therefore, breaks down for $\beta K < 2\pi$.
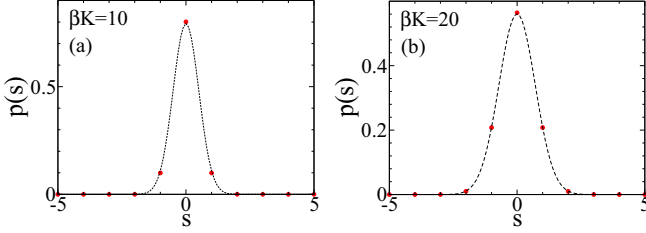
FIG. 8. Distributions $p(s)$ for a system Ξ_L at $\alpha = \alpha_c$, for (a) $\beta K = 10$ and (b) $\beta K = 20$. The discrete points are from a simulation and the continuous lines correspond to Eq. (58).

In Fig. 9 we plot $p(0)$ as a function of βK obtained from simulation for a discrete system and compare it to $p(0)$ calculated using Eq. (58).

Given the reliable performance of the approximation in the range $\beta K > 2\pi$, it is safe to conclude that there is no phase transition in this range. The distribution $p(s)$ is monomodal and its variance diverges only in the limit $\beta K \rightarrow \infty$. If there is any KT type of transition, then it must occur in the range $5 > \beta K > 6$ and can be associated with the emergence of the lone pairs in Fig. 7, which could be interpreted as the emergence of defects.

Because the MC simulations on the spin ensemble become impossible for $\beta K > 5$, since the only possible spins are $s_i = 0$, the KT transition along the βK parameter in the context of the two-component model could imply a different mechanism of the collapse transition.

V. FINITE ρ AND THE EMERGENCE OF A METASTABLE REGION

In this section we consider a more realistic situation where the average occupation number of a lattice site ρ is finite. This also means that the quadratic Hamiltonian H_∞ in Eq. (15) is modified by an additional nonquadratic term $h(s)$. A technical difficulty is that the system is no longer Gaussian and additional methods are needed to analyze it.

The simulations show that the thermodynamic collapse for finite ρ does not occur at $\alpha = 1/4$, as for the case $\rho \rightarrow \infty$, but is shifted to larger values of α. This indicates that the
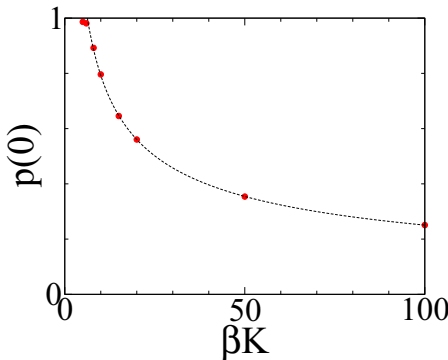

FIG. 9. The probability that a lattice site is empty, $p(0)$, as a function of βK. The data points are from simulation and the continuous line corresponds to $p(0)$ in Eq. (58).

thermodynamic collapse depends on density. This may be somewhat surprising, since one expects the global minimum of a system for $\alpha > 1/4$ to be a collapsed state. This indicates the presence of a metastable equilibrium.

In a two-component system, a collapsed configuration, as it emerges in a simulation, is composed of numerous clusters, each of which can, in principle, accommodate an infinite number of particles. A sequence of such clusters for a one-dimensional lattice model has been analyzed before [1]. Within a single cluster, a single site is occupied by one type of particles. (Similar clusters have been observed in a two-component system of penetrable spheres [3,4]). The energy of each cluster scales like $E \propto -n^2$, where n is the number of particles in a cluster.

If a collapsed configuration consists of a single cluster composed of all the particles in a system, then the energy of a collapsed state scales like $E \propto -n^2$ where n is the number of particles. The competing entropy of noncollapsed configurations, however, scales like $-ST \propto k_B T n \ln n$. This means that as soon as a configuration with energy that scales like $E \propto -n^2$ appears (which for the present model occurs when $\alpha > 1/4$), the global minimum will always be a collapsed state. The fact that the system does not collapse spontaneously when $\alpha > 1/4$ suggests that there is a local minimum that produces metastable equilibrium.

For a better grasp of the collapse mechanism, we describe a simple situation. We consider a finite system that roughly corresponds to a size of a cluster that emerges in a collapsed state. The system is in contact with a reservoir, so that a number of particles in the system n fluctuates. The particles in the reservoir do not interact with each other, while the energy of the system itself is assumed to be $\beta E = -an^2$ so that the system can achieve a collapsed configuration only if $a > 0$. The grand potential of the system is

$$\beta \Omega(n) = n \ln \frac{n}{2} - n - an^2 - \beta \mu n, \qquad (59)$$

where $n = n_+ + n_-$ is the total number of particles and $\frac{n}{2} \ln \frac{n}{2} - \frac{n}{2}$ is the entropy $-TS$ due to each species. If $a > 0$, then the global minimum of $\beta \Omega(n)$ is for $n = \infty$. However, there is also a local minimum $\frac{d\beta\Omega}{dn} = 0$, which yields

$$n_0 = -\frac{W(-4ae^{\beta\mu})}{2a} = 2e^{\beta\mu} + 8ae^{2\beta\mu} + \dots \qquad (60)$$

where n_0 corresponds to a metastable equilibrium. The local minimum vanishes for $a > \frac{1}{4e^{\beta\mu}}$ at which point the system collapses. Since the reservoir density is $\rho = e^{\beta\mu}$, we can establish the dependence of the critical value of a where the collapse occurs on the density as $a_c = \frac{1}{4\rho}$. We observe a similar qualitative behavior in simulations.

To use a more rigorous approach to analyze a metastable region, we start with a perturbation approximation. For a finite ρ, the system Hamiltonian is

$$H = H_\infty + \sum h(s_i). \qquad (61)$$

The partition function of this system can be written in terms of the H_∞ ensemble as [29]

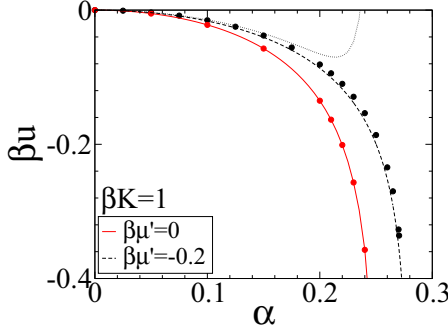$$\Xi = \Xi_\infty \langle e^{-\beta \sum h(s_i)} \rangle_\infty. \qquad (62)$$

FIG. 10. Internal energy (for indistinguishable particles) as a function of α for $\beta K = 1$, and $\beta\mu' = 0$ and $\beta\mu' = -0.2$. The data points are from Monte Carlo simulation. The solid line is for βu in Eq. (37). The dotted line incorporates the perturbative correction in Eq. (66). The dashed line is for the variational approach.

If we expand the quantity $\ln \Xi$, assuming h to be small, and keep only the first order term, then a perturbative expression is

$$\ln \Xi \approx \ln \Xi_\infty - \beta N \langle h(s) \rangle_\infty. \qquad (63)$$

Finally, if we use the separation $\Xi_\infty = \Xi_G \Xi_L$ and ignore discrete contributions, $\Xi_\infty \approx \Xi_G$, then we have

$$\ln \Xi \approx \ln \Xi_G - \beta N \langle h(s) \rangle_G, \qquad (64)$$

where the subscript G denotes the continuous Gaussian system analyzed earlier.

For indistinguishable particles $h(s_i) = -\mu'|s_i|$, where the average value of $|s_i|$ is related to A_{ii}^{-1}, see Eq. (A8), and the value of A_{ii}^{-1} is given in Eq. (53) for A_{ii}^{-1}, we get

$$\ln \Xi \approx \ln \Xi_G + \beta\mu' \frac{2N}{\pi} \sqrt{\frac{\mathrm{K}(16\alpha^2)}{\beta K}}. \qquad (65)$$

The internal energy per particle can now be obtained using the definition in Eq. (36). For $\beta\mu' < 0$, the expression in Eq. (37) is corrected as $u \to u + \Delta u$, where the correction due to the perturbation theory is given by

$$\beta\Delta u = \frac{\beta\mu'}{\pi} \sqrt{\frac{\mathrm{K}(16\alpha^2)}{\beta K}} \left[1 - \frac{1}{(1 - 16\alpha^2)} \frac{\mathrm{E}(16\alpha^2)}{\mathrm{K}(16\alpha^2)} \right], \quad (66)$$

where $\mathrm{E}(x)$ is the complete elliptic integral of the second kind.

Figure 10 plots the data points for βu, for $\beta K = 1$ and two values of the chemical potential, $\beta\mu' = 0$ and $\beta\mu' = -0.2$, the former corresponding to infinite and the latter to a finite density. The data points indicate that the reduced density leads to higher internal energy. The perturbative correction in Eq. (66) for the case $\beta\mu' = -0.2$ is shown as a dotted line. It accurately represents the simulated results for $\alpha < 0.15$, then for $\alpha > 0.15$ it becomes increasingly less accurate, and eventually diverges in the wrong direction as $\alpha \to 1/4$. Because the perturbation approach breaks down, it cannot tell us anything about the value of βu in a metastable region.
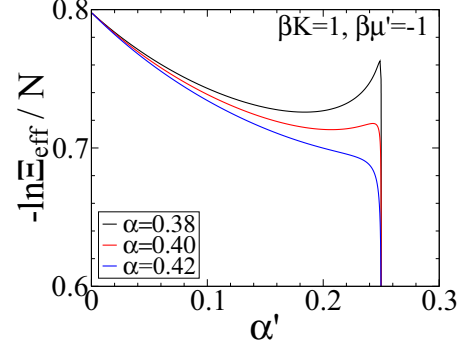

FIG. 11. $-\ln \Xi$ as a function of a variational parameter α' for $\beta K = 1$ and $\beta\mu' = -1$ (for indistinguishable particles), for three different values of α.

We next turn to a variational method. We start by postulating a quadratic auxiliary Hamiltonian,

$$H_\Gamma = \frac{K}{2} s^T \Gamma s,$$

where Γ is a $N \times N$ matrix. To keep things simple, it is assumed that Γ has the same structure as the matrix A, and the only difference is that the coupling constant does not correspond to a physical value α but is used as a variational parameter designated by α'. The partition function written in terms of the auxiliary ensemble is

$$\Xi = \left\langle e^{-\frac{\beta K}{2} s^T (A - \Gamma) s - \beta \sum h(s_i)} \right\rangle_\Gamma \Xi_\Gamma. \qquad (67)$$

Then, using the Gibbs-Bogoliubov-Feynman inequality (GBF) [29], we get

$$\Xi \geqslant e^{-\langle \frac{\beta K}{2} s^T (A - \Gamma) s - \beta \sum h(s_i) \rangle_\Gamma} \Xi_\Gamma, \qquad (68)$$

and the quantity $\ln \Xi$ becomes

$$\ln \Xi \geqslant \ln \Xi_\Gamma - \left\langle \frac{\beta K}{2} s^T (A - \Gamma) + N\beta h(s) \right\rangle_\Gamma. \qquad (69)$$

As the auxiliary system is Gaussian, the term in angular brackets can be evaluated, leading to

$$\ln \Xi \geqslant \ln \Xi_{\mathrm{eff}} = \ln \Xi_\Gamma + \beta\mu' \frac{2N}{\pi} \sqrt{\frac{\mathrm{K}(16\alpha'^2)}{\beta K}}$$
$$+ N \left(\frac{1}{2} - \frac{1}{\pi} \mathrm{K}(16\alpha'^2) \right) \left(1 - \frac{\alpha}{\alpha'} \right). \qquad (70)$$

Figure 11 plots $-\ln \Xi_{\mathrm{eff}}/N$, where $\ln \Xi_{\mathrm{eff}}$ is given in Eq. (70), as a function of a variational parameter α'. Because the plots are for $\alpha > 1/4$, the local minima in those plots correspond to metastable equilibriums. The minimum disappears at around $\alpha \approx 0.42$, in which case the system spontaneously collapses.

The free energy of a metastable equilibrium corresponds to the function $-\ln \Xi_{\mathrm{eff}}$ at a local minimum. The internal energy is subsequently obtained from the definition in Eq. (36). βu obtained in this way is shown in Fig. 10 for the parameters $\beta K = 1$ and $\beta\mu' = -0.2$ as a dashed line. Comparison with the exact results indicates high degree of accuracy of the variational approach.
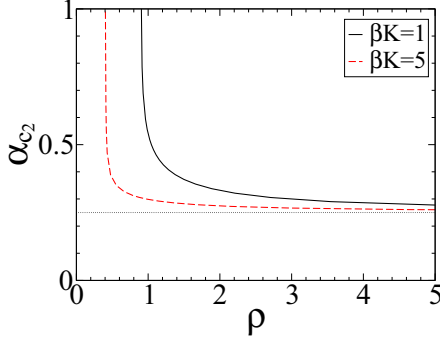
FIG. 12. Boundaries of the metastable region as a function of the particle density for indistinguishable particles. Global minimum corresponds to $\alpha = 1/4$ regardless of density. The metastable region extends above this value and strongly depends on density.

If we take the value of α where the local minimum of the function $-\ln \Xi_{\text{eff}}$ disappears, see Fig. 11, to indicate the end of the stability region, then we can use the variational method to obtain precise contours of the stability region.

Figure 12 plots such a boundary of the metastable region. To make contact with the original particle system, we plot the results as a function of a particle density. The density has been obtained from Eq. (10) and within the variational framework is given by

$$\rho = \sqrt{\frac{4\mathrm{K}\left(16\alpha'^2_0\right)}{\beta K \pi^2} + \frac{2e^{2\beta\mu'}}{1 - e^{2\beta\mu'}}}, \qquad (71)$$

where α'_0 corresponds to α' at a local minimum just as it is about to disappear. The results show drastic broadening of the metastable region as $\rho < 1$. This effect is even stronger for smaller βK.

For distinguishable particles we see the same type of general behavior and the emergence of the metastable region. However, the application of the variational procedure is more complex as the function $h(s)$ is more difficult to handle.

VI. CONCLUSION

This work investigates thermodynamic collapse in a two-component lattice-gas system of penetrable particles on a square-lattice substrate. Because particles are penetrable, there is no limit on how many particles occupy the same site, and the multiple occupation of a single site gives rise to different statistical mechanics, depending whether particles are regarded as distinguishable or indistinguishable. To facilitate analysis of the system, we transform the relevant partition function into the spin model with spins $s_i = 0, \pm 1, \pm 2, \dots$. In the limit $\rho \to \infty$, the system Hamiltonian recovers a simple quardatic form, so that the partition function corresponds to a discrete Gaussian model analyzed in the past in connection to interfaces and the roughening transition. The difference between the Gaussian model used to study interfaces and the Gaussian model of penetrable particles lies in the sign of interactions between spins. Because the Gaussian model at the point of a collapse becomes isomorphic with the lattice Coulomb system, we check for the existence of a KT phase transition along the line of the thermodynamic instability. The presence of the KT transition itself does not affect the collapse transition, it might, however, affect the mechanism.

To analyze the system for finite ρ we employ a variational approximation since for this situation the Hamiltonian is no longer harmonic. Both simulations and the approximation indicate the presence of a metastable equilibrium corresponding to a local minimum in the free energy. The extent of the metastable region furthermore strongly depends on density. The metastable region vanishes at an infinite density and diverges as density goes to zero.

APPENDIX A: SELECTED RELATIONS OF THE GAUSSIAN INTEGRAL

The partition function of a continuous Gaussian model is a Gaussian integral,

$$\Xi = \int_{-\infty}^{\infty} ds_1 \cdots \int_{-\infty}^{\infty} ds_N \, e^{-\frac{1}{2}s^T B s} = \sqrt{\frac{(2\pi)^N}{\det B}}, \qquad (A1)$$

where B is the $N \times N$ square and symmetric matrix and $s = (s_1, \dots, s_N)$ is the N-dimensional vector.

The probability that a spin i has a value s'_i can be obtained from the following definition:

$$p(s'_i) = \langle \delta(s_i - s'_i) \rangle. \qquad (A2)$$

Using the Fourier representation of a δ function, the relation above becomes

$$p(s'_i) = \frac{1}{2\pi} \int_{-\infty}^{\infty} dq \, \langle e^{iq(s_i - s'_i)} \rangle, \qquad (A3)$$

or, if we want to be more explicit,

$$p(s'_i) = \int_{-\infty}^{\infty} dq \frac{e^{-iqs'_i}}{2\pi \, \Xi} \left[\int_{-\infty}^{\infty} ds_1 \cdots \int_{-\infty}^{\infty} ds_N \, e^{iqs_i} e^{-\frac{1}{2}s^T B s} \right], \qquad (A4)$$

where the integral inside the square brackets is the Gaussian integral with the linear term which after evaluation leads to

$$p(s'_i) = \int_{-\infty}^{\infty} dq \frac{e^{-iqs'_i}}{2\pi} e^{-\frac{1}{2}q^2 B_{ii}^{-1}}, \qquad (A5)$$

which evaluates to

$$p(s_i) = e^{-\frac{s_i^2}{2B_{ii}^{-1}}} \sqrt{\frac{1}{2\pi B_{ii}^{-1}}}, \qquad (A6)$$

where B_{ii}^{-1} is the element of the inverse matrix B^{-1}. Using the distribution $p(s_i)$, the second moment of a spin s_i is

$$\langle s_i^2 \rangle_g = B_{ii}^{-1}. \qquad (A7)$$

We can also evaluate the average value of $|s_i|$,

$$\langle|s_i|\rangle_g = \sqrt{\frac{2B_{ii}^{-1}}{\pi}}. \tag{A8}$$

A similar procedure can be used to calculate a two-spin distribution function,

$$p(s_i', s_j') = \langle\delta(s_i - s_i')\delta(s_j - s_j')\rangle, \tag{A9}$$

for $i \neq j$. Using the Fourier representation of a δ function we get

$$p(s_i', s_j') = \left(\frac{1}{2\pi}\right)^2 \int_{-\infty}^{\infty} dq_1 \int_{-\infty}^{\infty} dq_2 \,\langle e^{iq_1(s_i - s_i')}e^{iq_2(s_j - s_j')}\rangle. \tag{A10}$$

If we follow similar steps taken to obtain $p(s_i')$, then we may obtain the expression for $p(s_i', s_j')$ which then allows us to calculate the spin-spin correlation function that evaluates to

$$\langle s_i s_j\rangle_g = B_{ij}^{-1}. \tag{A11}$$

Within the continuous Gaussian model, therefore, the inverse of the interaction matrix corresponds to the spin-spin correlation function.

APPENDIX B: MATRIX A FOR THE CONTINUOUS GAUSSIAN MODEL

In this section we obtain the matrix A of the continuous Gaussian model for an arbitrary dimension d. For the sake of concreteness, we assume the system size to be $L = 4$, and in $d = 1$ the system configuration can be represented with a vector

s_1	s_2	s_3	s_4

and the interaction matrix A for the periodic boundary conditions is

$$A_L = \begin{bmatrix} 1 & \alpha & 0 & \alpha \\ \alpha & 1 & \alpha & 0 \\ 0 & \alpha & 1 & \alpha \\ \alpha & 0 & \alpha & 1 \end{bmatrix}, \tag{B1}$$

where the subscript L denotes the matrix size $L \times L$. The matrix is circulant, symmetric, and real valued. Because only three elements are nonzero, the matrix, furthermore, is circulant tridiagonal.

In $d = 2$, the spins of the system with size $L = 4$ can be represented on a square grid as

s_1	s_2	s_3	s_4
s_5	s_6	s_7	s_8
s_9	s_{10}	s_{11}	s_{12}
s_{13}	s_{14}	s_{15}	s_{16}

and the resulting A matrix for the nearest-neighbor interactions is given by

$$A_{L^2} = \begin{bmatrix}
1 & \alpha & 0 & \alpha & \alpha & 0 & 0 & 0 & 0 & 0 & 0 & 0 & \alpha & 0 & 0 & 0 \\
\alpha & 1 & \alpha & 0 & 0 & \alpha & 0 & 0 & 0 & 0 & 0 & 0 & 0 & \alpha & 0 & 0 \\
0 & \alpha & 1 & \alpha & 0 & 0 & \alpha & 0 & 0 & 0 & 0 & 0 & 0 & 0 & \alpha & 0 \\
\alpha & 0 & \alpha & 1 & 0 & 0 & 0 & \alpha & 0 & 0 & 0 & 0 & 0 & 0 & 0 & \alpha \\
\alpha & 0 & 0 & 0 & 1 & \alpha & 0 & \alpha & \alpha & 0 & 0 & 0 & 0 & 0 & 0 & 0 \\
0 & \alpha & 0 & 0 & \alpha & 1 & \alpha & 0 & 0 & \alpha & 0 & 0 & 0 & 0 & 0 & 0 \\
0 & 0 & \alpha & 0 & 0 & \alpha & 1 & \alpha & 0 & 0 & \alpha & 0 & 0 & 0 & 0 & 0 \\
0 & 0 & 0 & \alpha & \alpha & 0 & \alpha & 1 & 0 & 0 & 0 & \alpha & 0 & 0 & 0 & 0 \\
0 & 0 & 0 & 0 & \alpha & 0 & 0 & 0 & 1 & \alpha & 0 & \alpha & \alpha & 0 & 0 & 0 \\
0 & 0 & 0 & 0 & 0 & \alpha & 0 & 0 & \alpha & 1 & \alpha & 0 & 0 & \alpha & 0 & 0 \\
0 & 0 & 0 & 0 & 0 & 0 & \alpha & 0 & 0 & \alpha & 1 & \alpha & 0 & 0 & \alpha & 0 \\
0 & 0 & 0 & 0 & 0 & 0 & 0 & \alpha & \alpha & 0 & \alpha & 1 & 0 & 0 & 0 & \alpha \\
\alpha & 0 & 0 & 0 & 0 & 0 & 0 & 0 & \alpha & 0 & 0 & 0 & 1 & \alpha & 0 & \alpha \\
0 & \alpha & 0 & 0 & 0 & 0 & 0 & 0 & 0 & \alpha & 0 & 0 & \alpha & 1 & \alpha & 0 \\
0 & 0 & \alpha & 0 & 0 & 0 & 0 & 0 & 0 & 0 & \alpha & 0 & 0 & \alpha & 1 & \alpha \\
0 & 0 & 0 & \alpha & 0 & 0 & 0 & 0 & 0 & 0 & 0 & \alpha & \alpha & 0 & \alpha & 1
\end{bmatrix}, \tag{B2}$$

where the size of the matrix is $L^2 \times L^2$. If we subdivide the matrix into equally sized square blocks, then we find three different submatrices. The diagonal blocks are identical to the matrix in Eq. (B1). The blocks adjacent to it are diagonal matrices with the diagonal element α, and the remaining blocks are zero matrices. The matrix A_{L^2} can more conveniently be represented as a $L \times L$ matrix whose elements in turn are $L \times L$ matrices,

$$A_{L^2} = \begin{bmatrix} A_L & \alpha I_L & 0_L & \alpha I_L \\ \alpha I_L & A_L & \alpha I_L & 0_L \\ 0_L & \alpha I_L & A_L & \alpha I_L \\ \alpha I_L & 0_L & \alpha I_L & A_L \end{bmatrix},$$

where I_L is an identity and 0_L is a zero square matrix. The block representation of the matrix A_{L^2} is a circulant matrix.

The block representation of the matrix A_{L^3} in $d = 3$ is

$$A_{L^3} = \begin{bmatrix} A_{L^2} & \alpha I_{L^2} & 0_{L^2} & \alpha I_{L^2} \\ \alpha I_{L^2} & A_{L^2} & \alpha I_{L^2} & 0_{L^2} \\ 0_{L^2} & \alpha I_{L^2} & A_{L^2} & \alpha I_{L^2} \\ \alpha I_{L^2} & 0_{L^2} & \alpha I_{L^2} & A_{L^2} \end{bmatrix}.$$

APPENDIX C: ONSAGER'S EXACT SOLUTION OF THE ISING MODEL

For an antiferromagnetic Ising model with the Hamiltonian

$$H = J \sum_{nn} s_i s_j, \tag{C1}$$

the free energy for a square-lattice geometry is given by [30]

$$\frac{\beta F}{N} = -\ln[2\cosh(2\beta J)]$$
$$- \frac{1}{8\pi^2} \int_0^{2\pi} dq_1 \int_0^{2\pi} dq_2 \, \ln[1 + 2\alpha \cos q_1 + 2\alpha \cos q_2],$$

where $N = L^2$ and

$$\alpha = \frac{1}{2} \frac{\sinh(2\beta J)}{\cosh^2(2\beta J)} \tag{C3}$$

is the function of the interaction strength. In view of the similarity of the integral term to that in Eq. (31), we may write

$$\frac{\beta F}{N} = -\ln[2\cosh(2\beta J)] + \frac{1}{4} \sum_{k=1}^{\infty} \frac{\alpha^{2k}}{k} \frac{(2k)!^2}{k!^4}, \tag{C4}$$

(recently, a similar expression, in terms of $_4F_3$ hyper- geometric function, has been obtained in [31]), and the partition function can be written as

$$\Xi_{IS} = [2\cosh(2\beta J)]^N \exp\left[-\frac{N}{4} \sum_{k=1}^{\infty} \frac{\alpha^{2k}}{k} \frac{(2k)!^2}{k!^4} \right]. \tag{C5}$$

Knowing that the series in the above expression has a convergence interval $|\alpha| \leqslant 1/4$, the phase transition must occur at $\alpha_c = 1/4$, on the edge of the stability region. Using Eq. (C3), this corresponds to

$$\frac{1}{2} \frac{\sinh(2\beta J_c)}{\cosh^2(2\beta J_c)} = \frac{1}{4}, \tag{C6}$$

which yields $\beta J_c = \ln(1 + \sqrt{2})/2$. (A number of interesting results for the Ising model in 2D based on series approach can be found in [32]).

APPENDIX D: CONNECTION WITH THE CHUI-WEEKS MODEL

The DG surface model of Chui and Weeks [15] can be represented by the following Hamiltonian:

$$H = \frac{J}{2} \sum_{j \neq i}^{N} \epsilon_{ij} (s_i - s_j)^2 + 4hJ \sum_{i=1}^{N} s_i^2, \tag{D1}$$

where $\epsilon_{ij} = 1$ if two spins are the nearest neighbors and $\epsilon_{ij} = 0$ otherwise. To connect the Chui-Weeks system to the quadratic Hamiltonian in Eq. (16) corresponding to the limit $\rho \to \infty$,

$$H_\infty = \frac{K}{2} \sum_{j \neq i}^{N} \alpha \epsilon_{ij} s_i s_j + \frac{K}{2} \sum_{i=1}^{N} s_i^2, \tag{D2}$$

we rewrite the above expression using $2s_i s_j = s_i^2 + s_j^2 - (s_i - s_j)^2$. This leads to

$$H_\infty = -\frac{K}{4} \sum_{j \neq i}^{N} \alpha \epsilon_{ij} (s_i - s_j)^2 + \frac{K}{2} \alpha \sum_{j \neq i}^{N} \epsilon_{ij} s_i^2 + \frac{K}{2} \sum_{i=1}^{N} s_i^2. \tag{D3}$$

Because in 2D there are four neighbors, this simplifies to

$$H_\infty = -\frac{\alpha K}{4} \sum_{j \neq i}^{N} \epsilon_{ij} (s_i - s_j)^2 + \frac{K}{2} (1 + 4\alpha) \sum_{i=1}^{N} s_i^2. \tag{D4}$$

By comparing the parameters of the Chui-Weeks model with the model governed by the Hamiltonian in Eq. (16) we get

$$J = -\frac{\alpha K}{2}, \quad h = -\frac{1 + 4\alpha}{4\alpha}.$$

For $\alpha = -1/4$, our model corresponds to the case $h = 0$, for which it becomes isomorphic with the lattice Coulomb model.

[1] D. Frydel and Y. Levin, Phys. Rev. E **98**, 062123 (2018).

[2] D. Frydel and M. Ma, Phys. Rev. E **93**, 062112 (2016).

[3] Y. Xiang and D. Frydel, J. Chem. Phys. **146**, 194901 (2017).

[4] D. Frydel and Y. Levin, J. Chem. Phys. **148**, 024904 (2018).

[5] D. Ruelle, *Statistical Mechanics: Rigorous Results* (Imperial-College Press, London, 1999).

[6] M. E. Fisher and D. Ruelle, J. Math. Phys. **7**, 260 (1966).

[7] D. M. Heyes and G. Rickayzen, J. Phys.: Condens. Matter **19**, 416101 (2007).

[8] C. N. Likos, Phys. Rep. **348**, 267 (2001).

[9] C. N. Likos, A. Lang, M. Watzlawek, and H. Löwen, Phys. Rev. E **63**, 031206 (2001).

[10] G. Malescio and S. Prestipino, Phys. Rev. E **92**, 050301(R) (2015).

[11] S. Prestipino and G. Malescio, Phys. A **457**, 492 (2016).

[12] G. Malescio, A. Parola, and S. Prestipino, J. Chem. Phys. **148**, 084904 (2018).

[13] Y. Levin, R. Pakter, F. B. Rizzato, T. N. Teles, and F. P. C. Benetti, Phys. Rep. **535**, 1 (2014).

[14] J. A. Cuesta and A. Sánchez, J. Stat. Phys. **115**, 869 (2004).

[15] S. T. Chui and J. D. Weeks, Phys. Rev. B **14**, 4978 (1976).

[16] J. D. Weeks, *Ordering in Strongly Fluctuating Condensed Matter Systems*, edited by T. Riste (Plenum Press, New York, NY, 1980), p. 293.

[17] K. Binder, *Cohesion and Structure of Surfaces*, (Elsevier, Amsterdam, 1995), edited by F. R. de Boer and D. G. Pettifor, Vol. 4, pp. 121–283.

[18] H. G. Ballesteros, L. A. Fernández, V. Martín-Mayor, A. Muñoz Sudupe, G. Parisi, and J. J. Ruiz-Lorenzoddag, Ising exponents in the two-dimensional site-diluted Ising model, J. Phys. A **30**, 8379 (1997).

[19] M. L. Rosinberg, *Liquid State Methods for Disordered Systems*, edited by C. Caccamo, J. P. Hansen, and G. Stell. New Approaches to Problems in Liquid State Theory. NATO Science Series (Series C: Mathematical and Physical Sciences), Vol 529. (Springer, Dordrecht, 1999).

[20] H. Chamati and S. Romano, First-order phase transitions in classical lattice-gas spin models, Phys. Rev. B **75**, 184413 (2007).

[21] E. Lubetzky, F. Martinelli, and A. Sly, Harmonic pinnacles in the discrete Gaussian model, Comm. Math. Phys. **344**, 673 (2016).

[22] M. Gitterman, *Phase Transitions: Modern Applications*, 2nd ed. (World Scientific Publishing, Singapore, 2014), p. 109, Sec. 8.3.

[23] D. C. Mattis, *The Theory of Magnetism Made Simple: An Introduction to Physical Concepts and to Some Useful Mathematical Methods*, 2nd ed. (World Scientific Publishing, Singapore, 2006), p. 378, Sec. 7.10.

[24] P. J. Davis, *Circulant Matrices* (John Wiley, New York, 1979).

[25] A. Kaveh and H. Rahami, Acta Mech. **217**, 51 (2011).

[26] M. Chen, SIAM J. Numer. Anal. **24**, 668 (1987).

[27] P. Gupta and S. Teitel, Phys. Rev. B **55**, 2756 (1997).

[28] F. Spitzer, *Principles of Random Walk*, 2nd. ed. (Springer, Princeton, New York, 2001), p. 151.

[29] D. Frydel, Eur. J. Phys. **36**, 065050 (2015).

[30] L. Onsager, Phys. Rev. **65**, 117 (1944).

[31] G. M. Viswanathan, J. Stat. Mech. (2015) P07004.

[32] Y. Chan, A. J. Guttmann, B. G. Nickel, and J. H. H. Perk, J. Stat. Phys. **145**, 549 (2011).